JOURNAL OF AGRICULTURAL AND FOOD CHEMISTRY

ARTICLE

pubs.acs.org/JAFC

Cinnamaldehyde Prevents Adipocyte Differentiation and Adipogenesis via Regulation of Peroxisome Proliferator-Activated Receptor-γ (PPARγ) and AMP-Activated Protein Kinase (AMPK) Pathways

Bo Huang, Hai Dan Yuan, Do Yeon Kim, Hai Yan Quan, and Sung Hyun Chung*

Department of Life and Nanopharmaceutical Science, College of Pharmacy, Kyung Hee University, Seoul 130-701, Republic of Korea

ABSTRACT: Cinnamaldehyde (CA), one of the active components of cinnamon, has been known to exert several pharmacological effects such as anti-inflammatory, antioxidant, antitumor, and antidiabetic activities. However, its antiobesity effect has not been reported yet. This study investigated the antidifferentiation effect of CA on 3T3-L1 preadipocytes, and the antiobesity activity of CA was further explored using high-fat-diet-induced obese ICR mice. During 3T3-L1 preadipocytes were differentiated into adipocytes, 10−40 μM CA was treated and lipid contents were quantified by Oil Red O staining, along with changes in the expression of genes and proteins associated with adipocyte differentiation and adipogenesis. It was found that CA significantly reduced lipid accumulation and down-regulated the expression of peroxisome proliferator-activated receptor-γ (PPAR-γ), CCAAT/enhancer-binding proteins α (C/EBPα), and sterol regulatory element-binding protein 1 (SREBP1) in concentration-dependent manners. Moreover, CA markedly up-regulated AMP-activated protein kinase (AMPK) and acetyl-CoA carboxylase (ACC), and these effects were blunted in the presence of AMPK inhibitor, compound C. In the animal study, weight gains, insulin resistance index, plasma triglyceride (TG), nonesterified fatty acid (NEFA), and cholesterol levels in the 40 mg/kg of CA-administered group were significantly decreased by 67.3, 55, 39, 31, and 23%, respectively, when compared to the high-fat diet control group. In summary, these results suggest that CA exerts antiadipogenic effects through modulation of the PPAR-γ and AMPK signaling pathways.

KEYWORDS: cinnamaldehyde, 3T3-L1 adipocytes, adipocyte differentiation, peroxisome proliferator-activated receptor γ, AMP-activated protein kinase

INTRODUCTION

The prevalence of obesity has rapidly increased in industrialized countries in the past few decades, most likely due to an overload in fat and/or refined carbohydrates and sedentary lifestyle. Obesity is associated with a number of diseases and metabolic abnormalities such as type 2 diabetes, hypertension, dyslipidemia, coronary heart disease, gallbladder disease, and some cancers.[1] Obesity treatment includes lifestyle changes, diet control, regular exercise, and pharmacotherapy as an adjunct. The history of pharmacotherapy for obesity, however, is not a great success story because most antiobesity drugs have been withdrawn from the market based on U.S. FDA warnings of serious adverse reactions. Recently, sibutramine was withdrawn from sale in the European Union in January 2010 due to increased risk of the development of heart problems.[2] Therefore, there is growing interest in herbal remedies due to the side effects associated with current antiobesity agents, because the plant kingdom is a wide field to search for natural effective antiobesity agents with slight or no side effects.

Cinnamon (bark of *Cinnamomum cassia*) is one of the oldest spices used in naturopathic medicine, cited in Chinese books 4000 years ago and traditionally used in Ayurvedic and Chinese medicine to treat diabetes.[3,4] Interest in this spice has increased since the discovery of its insulin-potentiating properties and initial findings illustrating cinnamon's ability to reduce fasting blood glucose and plasma lipids.[5−8] In overweight patients and women with polycystic ovary syndrome, nutritional intakes of cinnamon also improve insulin sensitivity and lead to beneficial antioxidant effects.[9,10] Cinnamaldehyde (CA) is one of the active components of cinnamon, and the essential oil of cinnamon is about 90% CA. However, there are no reports documenting an antiobesity effect of CA. The aim of this study was to investigate the inhibitory effect of CA on differentiation of 3T3-L1 preadipocytes and its action mechanism(s) and body weight lowering effect in mice fed a high-fat diet.

MATERIALS AND METHODS

Cell Culture and Adipocyte Differentiation. Mouse embryo fibroblasts 3T3-L1 cells were obtained from the American Type Culture Collection (Manassas, VA) and incubated in Dulbecco's modified Eagle's medium (Sigma-Aldrich, St. Louis, MO) containing 10% bovine calf serum and 100 U/mL penicillin−streptomycin at 37 °C and 5% CO_2 atmosphere. To induce differentiation, 2 days after confluence, preadipocytes (designated day 0) were cultured in differentiation medium (DM, 10% FBS, 10 μg/mL insulin, 0.5 mM isobutylmethylxanthine, and 1 μM dexamethasone) for 4 days, switched to post DM containing 10% FBS and 10 μg/mL insulin, and then changed to 10% FBS medium for an additional 2 days.

Cell Proliferation Assay. Cells (5×10^3 per 96 well) were incubated in the presence or absence of CA. After 48 and 96 h for 3T3-L1 preadipocytes or after 24 h for COS-7 cells, 20 μL of MTS

Received: December 15, 2010
Revised: March 14, 2011
Accepted: March 14, 2011
Published: March 14, 2011

ACS Publications © 2011 American Chemical Society

Table 1. Composition of the Experimental Diets

	RD 10% kcal		HFD 45% kcal	
	g %	kcal %	g %	kca l%
protein	19.2	20	24	20
carbohydrate	67.3	70	41	35
fat	4.3	10	24	45
total		100		100
kcal/g	3.85		4.73	

	RD 10% kcal		HFD 45% kcal	
ingredient	gm	kcal	gm	kcal
casein, 80 mesh	200	800	200	800
L-cystine	3	12	3	12
corn starch	315	1260	72.8	291
maltodextrin 10	35	140	100	400
sucrose	350	1400	172.8	691
cellulose, BW 200	50	0	50	0
soybean oil	25	225	25	225
lard	20	180	177.5	1598
Mineral Mix S10026	10	0	10	0
dicalcium phosphate	13	0	13	0
calcium carbonate	5.5	0	5.5	0
potassium citrate	16.5	0	16.5	0
Vitamin Mix V10001	10	40	10	40
choline bitartrate	2	0	2	0
FD&C yellow dye 5 (RD), red dye 40 (HFD)	0.05	0	0.05	0
total	**1055.05**	**4057**	**858.15**	**4057**

solution was added to each well, incubated for 30 min, and absorbance at 550 nm was measured using a microplate reader.

Oil Red O Staining. Oil Red O staining was performed on day 8. Briefly, cells were washed with phosphate-buffered saline (PBS) twice, fixed with 10% formalin for 30 min, and stained with Oil Red O for 1 h. Cells were photographed using a phase-contrast Olympus CKX41 microscope (Tokyo, Japan) in combination with a digital camera at 100× magnification. The stained lipid droplets were dissolved in isopropanol and quantified at 540 nm.

Determination of Glycerol-3-phosphate Dehydrogenase (GPDH) Activity. CA-treated 3T3-L1 adipocytes were harvested on day 8, washed twice with PBS, and collected with a scraper into 25 mM Tris buffer containing 1 mM EDTA and 1 mM DTT (pH 7.5). The harvested cells were sonicated in 25 ultrasonic bursts of 10 s, after which they were centrifuged at 10000 rpm for 5 min at 4 °C. The supernatants were assayed for GPDH activity using a commercial assay kit (Takara Bio, Shiga, Japan).

Luciferase Activity Assay. The reporter plasmids, kindly provided by Dr. Sang Hoon Kim of Kyung Hee University, were transfected into COS-7 cells using the Ex Gen 500 transfection reagent (Fermentas Inc., Glen Burnie, MD) according to the manufacturer's instruction. After transfection, cells were treated with pioglitazone (PPAR-γ agonist) in the absence or presence of CA for 24 h. At post-transfection luciferase activities were measured using the Dual-Luciferase Reporter Assay System (Promega, Madison, WI) using a GloMax20/20 luminometer (Turner Biosystems, Sunnyvale, CA).

Animal Treatment and Experimental Protocol. Animal study was reviewed and approved by the Institutional Animal Ethics Committee of Kyung Hee University. Five-week-old ICR mice (Orient Bio Inc., Seongnam-si, Korea) were housed in a temperature- (21 ± 2.0 °C) and humidity-controlled (50 ± 5%) room with a cycle of 12 h light/12 h darkness. ICR mice were randomly divided into four groups as follows: group fed a regular diet (RD); group fed a high-fat diet (HFD, Research Diets, New Brunswick, NJ); and treatment groups fed a high-fat diet plus CA at 20 mg/kg (CA20) or 40 mg/kg (CA40) (see Table 1). After 1 month, mice were anesthetized with diethyl ether after an overnight fast, and blood was drawn from the heart aorta into a vacuum tube; epididymal fat pads were removed, weighed, and frozen with liquid nitrogen.

Serum Chemistry Analysis. Plasma concentrations of glucose, triglyceride (TG), nonesterified fatty acid (NEFA), and cholesterol were determined using commercial kits (Stanbio Laboratory, Boerne, TX) and an automatic analyzer (SMARTLAB, Mannheim, Germany). The plasma insulin concentrations were determined using a mouse insulin enzyme immunoassay kit (Shibayagi, Gunma, Japan).

Histological Analysis. The epididymal fat pad was removed and fixed in 10% neutral buffered formalin. The fat pads were subsequently embedded in paraffin, sectioned in 5 μm thicknesses (Leica, Wetzlar, Germany), and stained with hematoxylin−eosin for microscopic assessment (Olympus, Tokyo, Japan). Three different cross-sectional areas and their cell populations were calculated using an image analysis program (Image-Pro Plus 6.0).

Reverse Transcription−Polymerase Chain Reaction (RT-PCR). Total RNA was extracted from the 3T3-L1 cells and epididymal fat tissue using the EASY-BLUE total RNA extraction kit (Intron Bio, Beverly, MA). cDNA synthesis was performed with 1 μg of total RNA, oligo (15)dT primers, and reverse transcriptase in a total volume of 50 μL. PCR reactions were performed in a total volume of 20 μL comprising 2 μL of cDNA product, 0.2 mM of each dNTP, 20 pmol of each primer, and 0.8 unit of Taq polymerase. Oligonucleotide primer sequences used in PCR amplification are as follows: actin, forward, 5′-GTCGTACCACTGGCATTGTG-3′, and reverse, 5′-GCCATCTCCTGCTCAAAGTC-3′; peroxisome proliferator-activated receptor-γ (PPAR-γ), forward, 5′-TTTTCAAGGGTGCCAGTTTC-3′, and reverse, 5′-AATCCTTGGCCCTCTGAGAT-3′; CCAAT/enhancer-binding proteins α (C/EBPα), forward, 5′-AGACATCAGCGCCTACATCG-3′, and reverse, 5′-TGTAGGTGCATGGTGGTCTG-3′; sterol regulatory element-binding protein 1 (SREBP1), forward, 5′-GCGCTACCGGTCTTCTATCA-3′, and reverse, 5′-TGCTGCCAAAAGACAAGGG-3′; adipocyte fatty acid binding protein (aP2), forward, 5′-AACACCGAGATTTCCTTCAA-3′, and reverse, 5′-TCACGCCTTTCATAACACAT-3′; fatty acid synthase (FAS), forward, 5′-GATCCTGGAACGAGAACAC-3′, and reverse, 5′-AGACTGTGGAACACGGTGGT-3′; stearoyl-coenzyme desaturase-1 (SCD-1), forward, 5′-CGAGGGTTGGTTGTTGATCTGT-3′, and reverse, 5′-ATAGCACTGTTGGCCCTGGA-3′; lipoprotein lipase (LPL), forward, 5′-TCCTCTGACATTTGCAGGTCTATC-3′, and reverse, 5′-GTGAATCCAGTTATGGGTTCCAC-3′; glycerol-3-phosphate acyltransferase (GPAT), forward, 5′-CCTGGGCATGATTGCAAAG-3′, and reverse, 5′-ACAGACTCCAGGTACCTGCTCAC-3′. PCR was performed at 95 °C for 30 s, followed by 58 °C (PPAR-γ, C/EBPα, SREBP1, LPL, actin), 50 °C (FAS), 56 °C (SCD-1), or 60 °C (aP2, GPAT) for 30 s and 72 °C for 1 min. The last cycle was followed by a final extension step at 72 °C for 10 min. The RT-PCR products were electophoresed in 0.8% agarose gels under 100 V and stained with 0.5 μg/mL ethidium bromide. Scanning densitometry was performed with an i-MAX Gel Image Analysis system (Core-Bio, Seoul, Korea).

Protein Extraction and Western Blot. 3T3-L1 cells and epididymal fat pads were homogenized in lysis buffer. Total proteins (30 μg) were separated by 8% SDS−polyacrylamide gel electrophoresis, transferred to a polyvinylidene difluoride membranes (Millipore, Billerica, MA), and then hybridized overnight at 4 °C with 1:1000 diluted pAMPK, AMPK, phospho-acetyl CoA carboxylase (pACC), and ACC

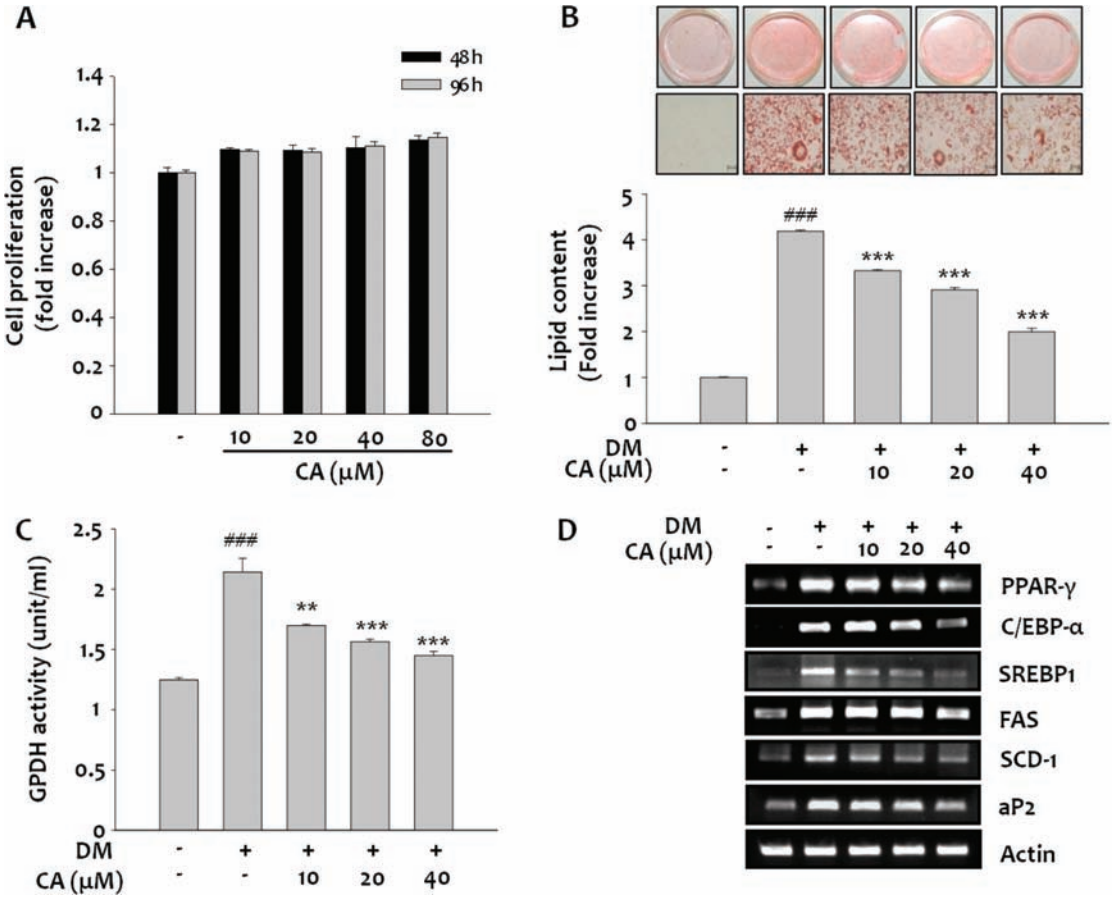

Figure 1. Effects of CA on adipogenesis in 3T3-L1 preadipocytes. (A) Cells were incubated with different concentrations of CA for 2 or 4 days. Cell proliferation was determined by MTS assay. (B) 3T3-L1 preadipocytes were treated with various concentrations of CA during differentiation. On day 8, cells were stained with Oil Red O and lipid contents were quantified by spectrophotometrically at 540 nm. (C) Glycerol-3-phosphate dehydrogenase (GPDH) activity was measured in the same experimental sets. (D) mRNA expression levels of PPAR-γ, C/EBPα, SREBP1c and its target molecules (FAS, SCD-1), and aP2 were estimated by RT-PCR. Each bar represents the mean ± SEM of thee independent experiments. ###, $p < 0.001$ compared with untreated cells; **, $p < 0.01$, and ***,$p < 0.001$, compared with differentiated cells.

primary antibodies (Cell Signaling, Beverly, MA). After incubation with 1:2000 diluted horseradish peroxidase-conjugated goat anti-rabbit or donkey anti-rabbit immunoglobulin G secondary antibody (Santa Cruz Biotechnology, Santa Cruz, CA) for 1 h at room temperature, immunoreactive proteins were visualized by an enhanced chemiluminescent solution (Amersham, Uppsala, Sweden) and quantified by a densitometric analysis.

Statistical Analysis. The results were represented as the mean ± SE. Comparison between groups was made by ANOVA variance analysis, and significance was analyzed by Tukey's test. Differences of $p < 0.05$ were considered to be statistically significant.

RESULTS

CA Prevents 3T3-L1 Preadipocyte Differentiation. First, we investigated the effect of CA on the proliferation of 3T3-L1 cells by MTS assay. Growth profiles observed at the second and fourth days of culture in the presence of indicated concentrations of CA were similar to that of the control, suggesting that CA did not show any cytotoxicity at up to 80 μM (Figure 1A). To examine the effect of CA on differentiation of preadipocytes into adipocytes, confluent 3T3-L1 preadipocytes were treated with the indicated concentrations of CA for 4 days. On the eighth day of incubation, lipid accumulation as a marker of differentiation was examined by Oil Red O staining. Triglycerides presented in fully differentiated adipocytes were stained with Oil Red O solution, and the lipid contents measured at 540 nm were concentration-dependently decreased (Figure 1B). To further characterize the antidifferentiation activity of CA, the cellular GPDH enzyme activity was measured, because the cytosolic GPDH plays an important role in the synthesis of triglyceride.[11] As shown in Figure 1C, CA suppressed the GPDH activity in a concentration-dependent manner. Next, to investigate whether reduced lipid contents and GPDH activity resulted from CA-mediated alteration in the differentiation program, the expression of transcription factors for adipogenesis was examined using RT-PCR. As shown in Figure 1D, the mRNA levels of PPAR-γ and C/EBPα were reduced in concentration-dependent fashions. We also found that CA significantly reduced the mRNA levels of SREBP1, target genes (FAS and SCD-1), and aP2.

CA Inhibits PPAR-γ Transcriptional Activity. First, we investigated the effect of CA on the proliferation of COS-7 cells by MTS assay. Growth profiles observed after 24 h culture in the presence of indicated concentrations of CA were similar to that of the control, suggesting that CA did not show any cytotoxicity at up to 80 μM (Figure 2A). To examine whether CA could

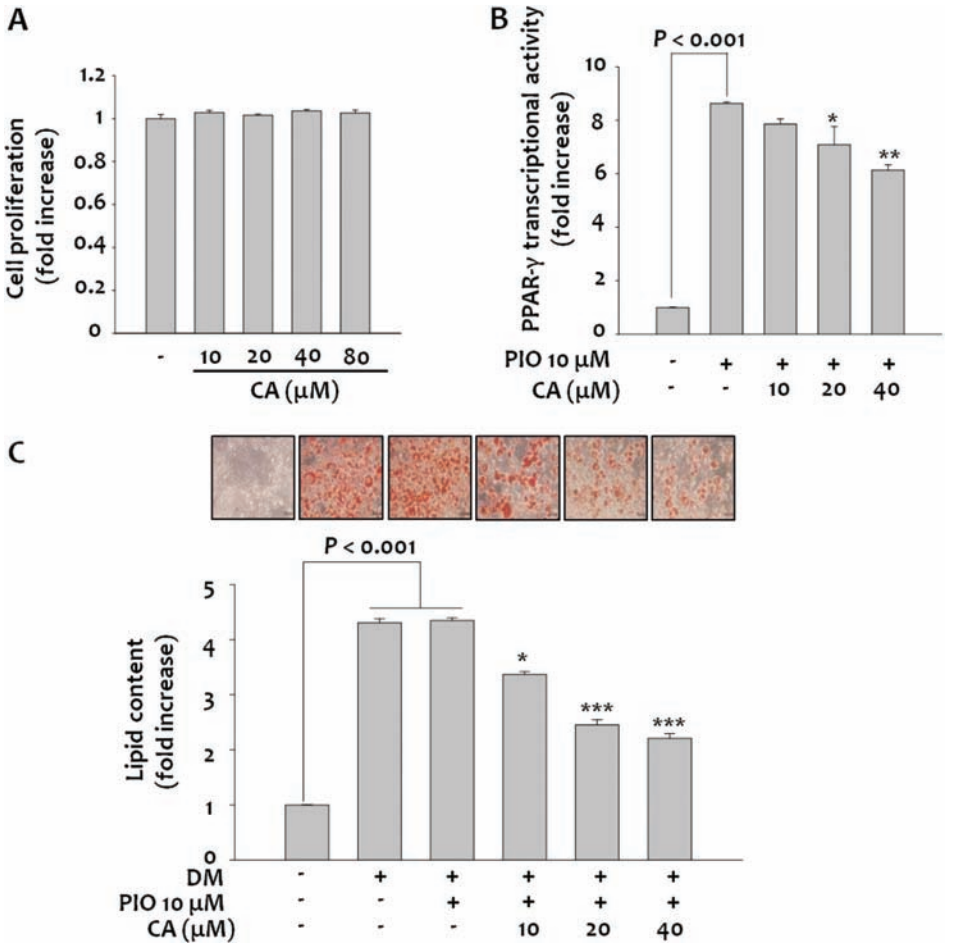

Figure 2. Effects of CA on PPAR-γ transcriptional activity. (A) Cells were incubated with different concentrations of CA for 1 day. Cell proliferation was determined by MTS assay. (B) PPAR-γ and RXRα were cotransfected with PPRE-luciferase reporter construct into cos-7 cells for 24 h. The cells were treated with pioglitazone in the absence or presence of CA. After 24 h, luciferase activity was assayed. (C) Differentiating 3T3-L1 cells were treated with CA at various concentrations in the presence of pioglitazone and stained with Oil Red O, and lipid contents were quantified. These experiments were conducted as independent experiments in triplicate. Data represent the mean ± SEM. *, $p < 0.05$, **, $p < 0.01$, and ***, $p < 0.001$, compared with pioglitazone-treated cells.

suppress the transcriptional activity of PPAR-γ, full-length PPAR-γ expression plasmid was transfected into COS-7 cells for the luciferase reporter gene assay. As shown in Figure 2B, CA significantly inhibited the pioglitazone-induced PPAR-γ transcriptional activity. Next, we performed a competitive inhibition assay using a strong PPAR-γ agonist, pioglitazone, in the adipocyte differentiation process. Remarkably, CA suppressed adipocyte differentiation even in the presence of pioglitazone, as shown by Oil Red O staining, and lipid contents were also markedly lowered (Figure 2C). These results indicate that CA prevents adipocyte differentiation through an antagonistic effect on PPAR-γ transcriptional activity.

Effects of CA on AMPK and Its Target Gene Expression. AMPK is known to play a major role in glucose and lipid metabolism and to control metabolic disorders such as diabetes, obesity, and cancer.[12] To test whether CA affects the AMPK signaling pathway, 3T3-L1 adipocytes were treated with three different concentrations of CA. Phosphorylated forms of AMPK and its immediate substrate (ACC) were significantly induced, and these effects were blunted in the presence of compound **C**, a specific inhibitor of AMPK (Figure 3A,B). Lipid contents in fat droplet were also regained in the presence of compound **C**, as shown in Figure 3D, suggesting that AMPK signaling pathway is associated with adipogenesis in 3T3-L1 cells. As expected, gene expressions of SREBP1 and FAS, downstream genes for AMPK, were decreased by CA treatment, and these effects were reversed in the presence of compound **C**. However, gene expressions of PPAR-γ and C/EBPα were not changed in the presence of compound **C**, indicating that these transcription factors and the AMPK signal pathway might be involved in the adipocyte differentiation and adipogenesis, respectively (Figure 3C).

Effects of CA on Body Weight and Metabolic Parameters. Body weight was measured once a week. Weight gains in RD and HFD control groups during the 4 week period were 0.8 ± 0.2 g (2.5% increase over the initial body weight) and 10.4 ± 2.2 g (33% increase over the initial body weight), respectively (Table 2). However, weight gains in CA-treated groups were significantly lowered when compared to HFD control group, decreased by 38.5% in the CA20 group and by 67.3% in the CA40 group. In the meantime, CA did not affect on food and water intakes. Feed efficiency was calculated by weight gain divided by total food intake for the 4 week period, and the high feed efficiency shown in the HFD-fed control group was dose-dependently reduced in the CA-treated groups. The effects of CA on plasma glucose, insulin, and lipid levels were also

dx.doi.org/10.1021/jf104814t |*J. Agric. Food Chem.* 2011, 59, 3666–3673

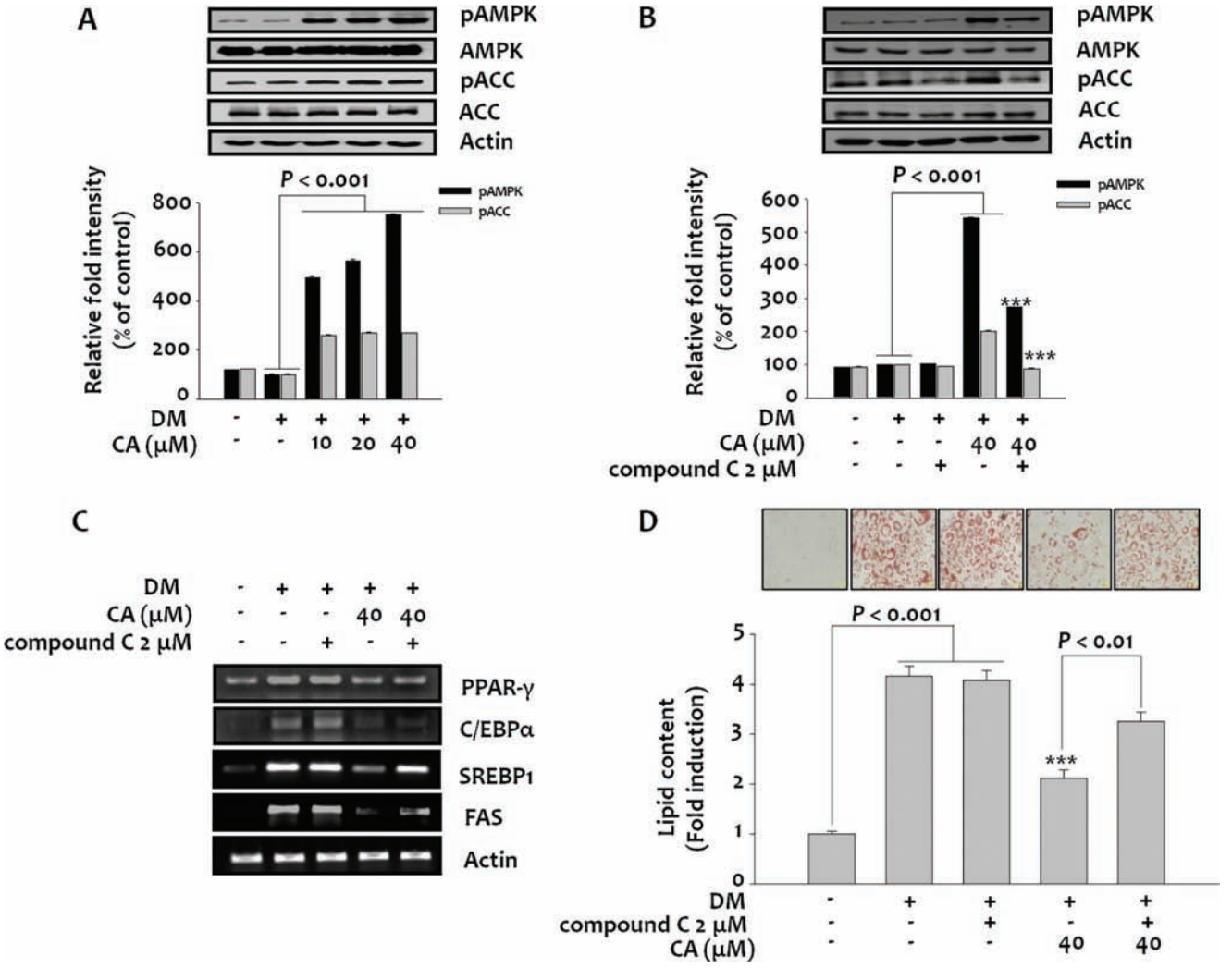

Figure 3. Effects of CA on phosphorylation of AMPK and ACC during 3T3-L1 differentiation. 3T3-L1 preadipocytes were differentiated in the presence of CA (0, 10, 20, and 40 μM) for 8 days. (A) Immunoblot analysis for pAMPK and pACC was described under Materials and Methods. (B, D) 3T3-L1 cells were treated with CA in the presence or absence of compound **C**. Cells were stained with Oil Red O at 8 days, and lipid contents were quantified. These experiments were conducted as independent experiments in triplicate. Data represent the mean ± SEM. ***, $p < 0.001$ compared with differentiated cells; ##, $p < 0.01$ compared with CA treated differentiation cells. (C) 3T3-L1 cells were treated with CA during differentiation in the presence or absence of compound **C**. The mRNA expression levels of PPAR-γ, C/EBPα, SREBP1c, and FAS were examined by RT-PCR.

examined at the end of treatment. Plasma glucose and insulin levels were increased by 1.5- and 2.7-fold in the HFD group compared to those in the RD group. CA-treated mice, however, showed significantly lowered plasma glucose and insulin levels in concentration-dependent manners. With increased plasma glucose and insulin levels, homeostasis model assessment for insulin resistance (HOMA-IR) value[13] of the HFD group was 3.9 times higher than that of the RD group. However, these values for the CA20 and CA40 group were significantly reduced by 24% ($p < 0.05$) and 55% ($p < 0.001$), respectively, when compared to the HFD group. The plasma lipid levels in the HFD control mice were significantly increased compared to those in the RD control mice: 1.6-, 1.5- and 1.7-fold increase for TG, NEFA, and cholesterol, respectively. However, the CA20 and CA40 groups showed considerably reduced levels of TG, NEFA, and cholesterol (39, 31, and 23% inhibition in the CA40 group).

Effects of CA on Epididymal Fat Morphology and Gene Expression for Adipogenesis. The body weight of HFD control mice was increased by 31% when compared to RD control mice (Table 2). Notably, histological analysis of epididymal fat pad confirmed this result and indicated that the number of cells of bigger size was markedly increased in the HFD control mice. On the other hand, the number of cells of 1000−10000 μm^2 was decreased by 39 and 68% in the CA20 and CA40 groups, respectively (Figure 4A,B). Parallel to in vitro assay, we examined gene and protein expressions responsible for lipogenesis and lipolysis in the epididymal fat tissue. As shown in Figure 4C, gene expressions of PPAR-γ, C/EBPα, SREBP1, FAS, SCD-1, aP2, LPL, and GPAT were all decreased in CA-treated mice when compared to those in HFD control mice in dose-dependent manners. In contrast, phosphorylated forms of AMPK and ACC, responsible for fatty acid β-oxidation, were markedly induced in CA-treated mice (Figure 4D).

DISCUSSION

Cinnamon has been used as a spice and traditional herbal medicine for centuries. The in vitro and in vivo evidence suggest

Table 2. Metabolic Parameters in Vehicle or CA-Treated ICR Mice

			HFD + CA (mg/kg)	
parameter	RD	HFD	20	40
initial body weight (g)	31.3 ± 1.6	31.7 ± 1.1	31.6 ± 1.7	31.7 ± 1.2
final body weight (g)	32.1 ± 2.0	42.1 ± 2.1†††	38.0 ± 1.4**	35.1 ± 3.0***
weight gain (g)	0.8 ± 0.2	10.4 ± 2.2†††	8.9 ± 2.3*	3.4 ± 3.3**
feed efficiency	0.01 ± 0.01	0.09 ± 0.02†††	0.07 ± 0.03	0.02 ± 0.02**
plasma glucose (mM)	4.8 ± 1.7	7.3 ± 0.7†††	5.7 ± 1.6	4.8 ± 1.5***
plasma insulin (μU/mL)	60.2 ± 4.1	162.7 ± 9.3†††	138.6 ± 5.1*	96.4 ± 6.9***
HOMA-IR	13.5 ± 1.3	52.3 ± 3.9†††	39.8 ± 5.5*	23.6 ± 2.5***
plasma lipids				
TG (mg/mL)	89.0 ± 0.3	142.7 ± 8.8†††	107.0 ± 4.3**	89.3 ± 4.9***
NEFA (μequiv/L)	880.3 ± 45.9	1357.0 ± 16.6†††	1207.8 ± 71.5*	936.0 ± 38.9***
cholesterol (mg/mL)	106.3 ± 2.7	182.0 ± 3.6†††	151.7 ± 5.5**	141.3 ± 5.6***

[a] Values are the mean ± SE (n = 6). RD, regular diet; HFD, high-fat diet; HFD + CA, HFD plus CA treatment. †††, $p < 0.001$ vs RD; *, $p < 0.05$; **, $p < 0.01$; ***, $p < 0.001$ vs HFD.

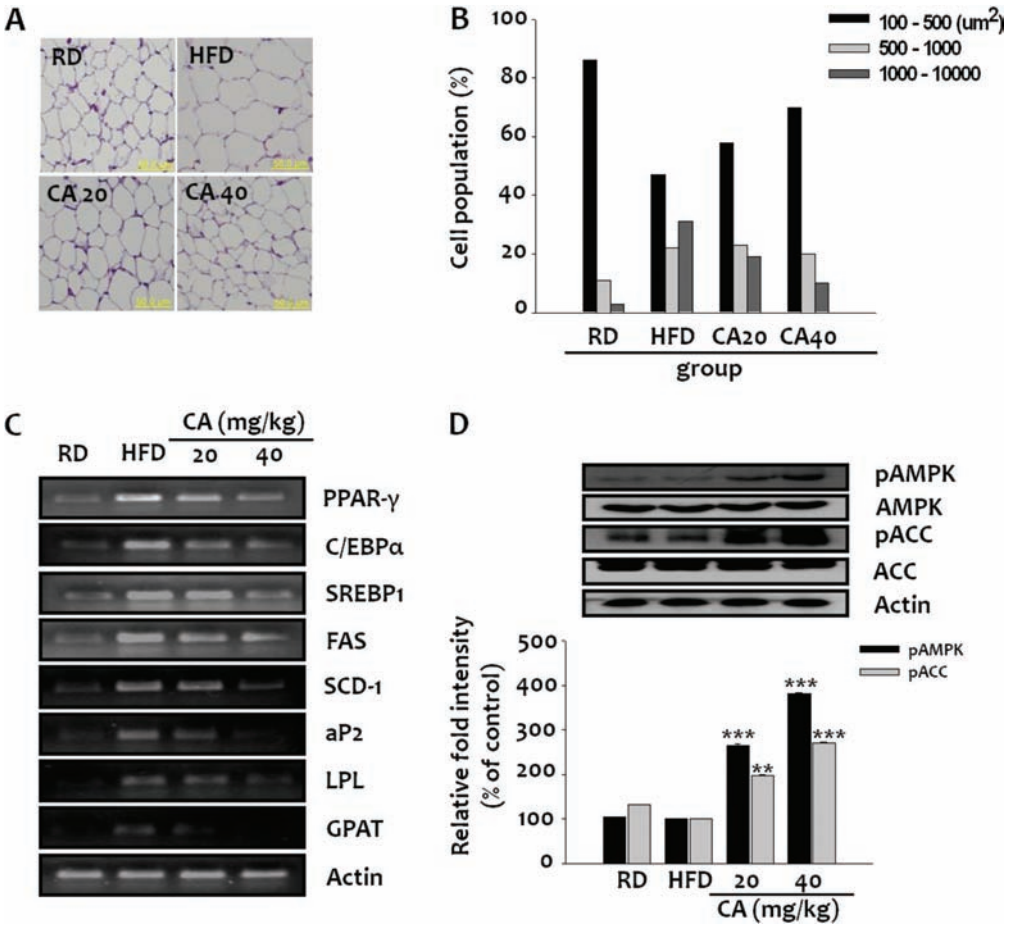

Figure 4. Effects of CA on morphology and gene and protein expression in the epididymal fat. (A) Epididymal fat pad was stained with hematoxylin-eosin, and microscopic pictures were obtained at magnification of ×200. (B) Three different cross-sectional areas and their cell populations were calculated using an image analysis program. (C) RT-PCR analyses of PPAR-γ, C/EBPα, SREBP1c and its target genes (FAS, SCD-1, GPAT), aP2, and LPL mRNA expression in epididymal tissue. (D) p-AMPK and p-ACC protein expression in epididymal tissue was determined by Western blot analyses.

that cinnamon has anti-inflammatory, antimicrobial, antioxidant, antitumor, plasma cholesterol and glucose-lowering, and immune-modulatory effects.[14] Two medicinal herbs of the genus *Cinnamomum*, *C. cassia* and *C. zeylanicum*, are generally approved,[15] and the bark is the only part of these plants that is used as a spice or for medical purposes (*Cinnamomi cortex*). The volatile oils obtained from the bark, leaf, and root-bark of *C. zeylanicum* and *C. cassia* vary significantly in chemical

composition,[16] and these oils of three different plant parts possess the same array of monoterpene hydrocarbons in different proportions. However, each oil has a different primary constituent: cinnamaldehyde (in the bark oil), eugenol (in the leaf oil), or camphor (in the root-bark oil). Among these primary constituents, CA is of particular interest. Although CA has been known to exert several pharmacological effects such as anti-inflammatory, antioxidant, antimicrobial, and antidiabetic activities,[17−20] its antiobesity effect has not been reported yet. Here, we investigated the antidifferentiation effect of CA on 3T3-L1 preadipocytes, and the antiobesity activity of CA was further explored using high-fat-diet-induced obese ICR mice.

The exact mechanisms of CA's lipid-modulating effects are not fully understood; however, we found that CA significantly down-regulated the transcription factors such as PPAR-γ, C/EBPα, and SREBP1 (Figure 1D) and up-regulated the AMPK and ACC (Figure 3A). The nuclear receptor PPAR-γ and members of C/EBPα synergistically activate the downstream promoters of adipocyte-specific genes such as aP2, FAS, LPL, GPAT, and SCD-1.[21] CA down-regulated the expression of PPAR-γ and C/EBP levels, which may be the mechanism that prevented HFD-fed ICR mice from gaining weight. In addition, CA directly inhibited the PPAR-γ transcriptional activity and preadipocyte differentiation in concentration-dependent manners (Figure 2B, C). The antiobesity effect of CA may be partially ascribed to not only down-regulation of PPAR-γ and C/EBPα levels but also direct PPAR-γ antagonistic action.

Major causes of the metabolic disorder include overweight, physical inactivity, and high-carbohydrate diet that cause the disturbance of energy metabolism. A variety of metabolic diseases are highly associated with insulin resistance, the causes of which are genetic, and environmental factors including obesity and physical fitness.[22] Because treatment of insulin resistance has beneficial effects on diabetes, dyslipidemia, obesity, and atherosclerosis, AMPK emerges as a therapeutic target for metabolic disorders.[23] AMPK is involved in the maintenance of lipid and cholesterol homeostasis; it stimulates the β-oxidation of fatty acids in mitochondria for lipid utilization. AMPK inhibits the activity of ACC though phosphorylation. Under normal conditions, inhibition of ACC by AMPK through phosphorylation leads to a fall in malonyl-CoA content and a subsequent decrease in fatty acid synthesis and increase in mitochondrial fatty acid oxidation via the allosteric regulation of carnitine palmitoyltransferase-1 (CPT-1), which catalyzes the entry of long-chain fatty acyl-CoA into mitochondria. Inactivation of ACC by AMPK helps promote fatty acid utilization, leading to fat burning in fat and muscle. As shown in Figure 3A, CA stimulated AMPK and ACC phosphorylations in dose-dependent fashions. In addition, these phosphorylations were significantly attenuated in the presence of compound **C**, an AMPK inhibitor (Figure 3B). The role of AMPK in lipolysis is complex. However, recent data showed that (i) activation of AMPK through a cAMP-dependent mechanism is required for activation of lipolysis in 3T3-L1 cells,[24] (ii) AMPK modulates adrenaline-induced lipolysis in isolated adipocytes,[25] and (iii) AMPK stimulates lipolysis in adipocytes via phosphorylation of hormone-sensitive lipase.[26] Thus, CA inhibited fatty acid synthesis and may stimulate lipolysis via activation of AMPK.

The fact that AMPK signaling might be associated with an adipocyte differentiation program is still controversial, but we found that preadipocyte 3T3-L1 cells were not able to develop to mature adipocytes in the presence of CA and that this effect was reversed when the cells were pretreated with compound **C**, an AMPK inhibitor (Figure 3D). In the meantime, CA-induced down-regulations of PPAR-γ and C/EBPα were not recovered in the presence of compound **C**, as shown in Figure 3C. These results suggest that transcription factors such as PPAR-γ and C/EBPα are responsible for adipocyte differentiation and AMPK signaling is responsible for inhibition of maintenance of adipocyte differentiation and fat accumulation. Although modulations of AMPK and PPAR-γ signaling might be responsible for the antiobesity effect of CA, cross talk between them was not found (Figure 3C).

In summary, our study demonstrated that CA significantly reduces the body weight and feed efficiency and improves insulin sensitivity in HFD-induced obese ICR mice. Moreover, CA reduces serum TG, NEFA, and cholesterol, thereby regulating lipid metabolism. On the basis of in vitro and in vivo studies, CA altered the expression of many genes that are involved in adipocyte differentiation and adipogenesis. These results provide molecular information for further investigation of the mechanisms by which CA moderates lipid metabolism. Furthermore, these results could be important in devising mechanism-based therapeutic strategies for lipid disorders such as obesity and dyslipidemia.

AUTHOR INFORMATION

Corresponding Author

*Phone: 822-961-0373. Fax: 822-957-0384. E-mail: suchung@khu.ac.kr.

Funding Sources

We acknowledge the support of this study by the Bio R&D program through the National Research Foundation of Korea funded by the Ministry of Education, Science and Technology (Grant 2009-0092562).

REFERENCES

(1) Medina-Gomez, G.; Vidal-Puig, A. Gateway to the metabolic syndrome. *Nat. Med.* **2005**, *11*, 602–603.

(2) Hsu, Y. W.; Chu, D. C.; Ku, P. W.; Liou, T. H.; Chou, P. Pharmacotherapy for obesity: past, present and future. *J. Exp. Clin. Med.* **2010**, *2*, 118–123.

(3) Qin, B.; Nagasaki, M.; Ren, M.; Bajotto, G.; Oshida, Y.; Sato, Y. Cinnamon extract (traditional herb) potentiates *in vivo* insulin-regulated glucose utilization via enhancing insulin signaling in rats. *Diabetes Res. Clin. Pract.* **2003**, *62*, 139–148.

(4) Modak, M.; Dixit, P.; Londhe, J.; Ghaskadbi, S.; Devasagayam, T. P. A. Indian herbs and herbal drugs used for the treatment of diabetes. *J. Clin. Biochem. Nutr.* **2007**, *40*, 163–173.

(5) Khan, A.; Bryden, N. A.; Polansky, M. M.; Anderson, R. A. Insulin potentiating factor and chomium content of selected foods and spices. *Biol. Trace Elem. Res.* **1990**, *24*, 183–188.

(6) Khan, A.; Safdar, M.; Khan, M.; Khattak, K. N.; Anderson, R. A. Cinnamon improves glucose and lipids of people with type 2 diabetes. *Diabetes Care* **2003**, *26*, 3215–3218.

(7) Lee, J. S.; Jeon, S. M.; Park, E. M.; Huh, T. L.; Kwon, O. S.; Lee, M. K.; Choi, M. S. Cinnamate supplementation enhances hepatic lipid metabolism and antioxidant defense systems in high cholesterol-fed rats. *J. Med. Food* **2003**, *6*, 183–191.

(8) Kannappan, S.; Jayaraman, T.; Rajasekar, P.; Ravichandran, M. K.; Anuradha, C. V. Cinnamon bark extract improves glucose metabolism and lipid profile in the fructose-fed rat. *Singapore Med. J.* **2006**, *47*, 858–863.

(9) Ziegenfuss, T. N.; Hofheins, J. E.; Mendel, R. W.; Landis, J.; Anderson, R. A. Effects of a water-soluble cinnamon extract on body composition and features of the metabolic syndrome in pre-diabetic men and women. *J. Int. Soc. Sports Nutr.* **2006**, *28*, 45–53.

(10) Wang, J. G.; Anderson, R. A.; Graham, G. M., 3rd; Chu, M. C.; Sauer, M. V.; Guarnaccia, M. M.; Lobo, R. A. The effect of cinnamon extract on insulin resistance parameters in polycystic ovary syndrome: a pilot study. *Fertil. Steril.* **2007**, *88*, 240–243.

(11) Kozak, L. P.; Jesen, J. T. Genetic and developmental control of multiple forms of L-glycerol 3-phosphate dehydreogenase. *J. Biol. Chem.* **1974**, *249*, 7775–7781.

(12) Carling, D. The AMP-activated protein kinase cascade − a unifying system for energy control. *Trends Biochem. Sci.* **2004**, *29*, 18–24.

(13) Matthews., D. R.; Hosker, J. P.; Rudenski, A. S.; Naylor, B. A.; Treacher, D. F.; Turner, R. C. Homeostasis model assessment: insulin resistance and beta-cell function from fasting plasma glucose and insulin concentrations in man. *Diabetologia* **1985**, *28*, 412–419.

(14) Teuscher, E. Zimt. In *Gewürzdrogen*; Wissenschaftliche Verlagsgesellschaft: Stuttgart, Germany: 2003; pp 423−429.

(15) ESCOP. In *Cinnamomi Cortex*, 2nd ed.; ESCOP Monographs; Thieme: Exeter, U.K., 2003; pp 92−97.

(16) Shen, Q.; Chen, F.; Luo, J. Comparison studies on chemical constituents of essential oil from ramulus *cinnamomi* and cortex *cinnamomi* by GC-MS. *Zhong Yao Cai* **2002**, *25*, 257–258.

(17) Chao, L. K.; Hua, K. F.; Hsu, H. Y.; Cheng, S. S.; Lin, I. F.; Chen, C. J.; Chen, S. T.; Chang, S. T. Cinnamaldehyde inhibits pro-inflammatory cytokines secretion from monocytes/ macrophages though suppression of intracellular signaling. *Food Chem. Toxicol.* **2007**, *46*, 220–231.

(18) Gowder, S. J.; Devaraj, H. Effect of the food flavour cinnamaldehyde on the antioxidant status of rat kidney. *Basic Clin. Pharmacol. Toxicol.* **2006**, *99*, 379–382.

(19) Pei, R. S.; Zhou, F.; Ji, B. P.; Xu, J. Evaluation of combined antibacterial effects of eugenol, cinnamaldehyde, thymol, and carvacrol against E. coli with an improved method. *J. Food Sci.* **2009**, *74*, 379–383.

(20) Zhang, W.; Xu, Y. C.; Guo, F. J.; Meng, Y.; Li, M. L. Anti-diabetic effects of cinnamaldehyde and berberine and their impacts on retinol-binding protein 4 expression in rats with type 2 diabetes mellitus. *Chin. Med. J.* **2008**, *121*, 2124–2128.

(21) Rosen, E. D.; MacDougald, O. A. Adipocyte differentiation from the inside out. *Nat. Rev. Mol. Cell Biol.* **2006**, *7*, 885–896.

(22) Bogardus, C.; Lillioja, S.; Mott, D. M.; Hollenbeck, C.; Reaven, G. Relationship between degree of obesity and in vivo insulin action in man. *Am. J. Physiol.* **1985**, *248*, 286–291.

(23) Zhang, B. B.; Zhou, G.; Li, C. AMPK: an emerging drug target for diabetes and the metabolic syndrome. *Cell Metab.* **2009**, *9*, 407–416.

(24) Yin, W.; Mu, J.; Birnbaum, M. J. Role of AMP-activated protein kinase in cyclic AMP-dependent lipolysis in 3T3-L1 adipocytes. *J. Biol. Chem.* **2003**, *278*, 43074–43080.

(25) Koh, H. J.; Hirshman, M. F.; He, H.; Li, Y.; Manabe, Y.; Balschi, J. A.; Goodyear, L. J. Adrenaline is a critical mediator of acute exercise-induced AMP-activated protein kinase activation in adipocytes. *Biochem. J.* **2007**, *403*, 473–481.

(26) Smith, A. J.; Thompson, B. R.; Sanders, M. A.; Bernlohr, D. A. Interaction of the adipocyte fatty acid-binding protein with the hormone-sensitive lipase; regulation by fatty acids and phosphorylation. *J. Biol. Chem.* **2007**, *282*, 32424–32432.